Surface Review and Letters, Vol. 9, Nos. 5 & 6 (2002) 1803–1808
© World Scientific Publishing Company

GROWTH EQUATIONS, DISCRETE MODELS AND MBE EXPERIMENTS

J. R. SÁNCHEZ, D. A. MIRABELLA and C. M. ALDAO*
Institute of Materials Science and Technology (INTEMA),
Universidad Nacional de Mar del Plata–CONICET,
Juan B. Justo 4302, 7600 Mar del Plata, Argentina
**cmaldao@mdp.edu.ar*

The question of the validity of the scaling ansatz in discrete deposition models and their connection with the scaling exponents of continuum differential equations is addressed. We specifically focus on the scaling properties of the Wolf–Villain type models and, as an extension of this model, on the influence of attractive and repulsive interactions up to second neighbors on the scaling relation. As an example of technological relevance, we present the evolution of steps in the vicinal (100) surface of Si during deposition at relatively low temperatures. We have found that, in general, one should not expect that discrete models, as well as real crystals, exhibit scaling.

1. Introduction

In the last two decades, kinetic roughening of interfaces growing far from equilibrium has become of great interest.[1–3] From a theoretical point of view, growth processes have been described using both discrete models and continuum equations. It has been argued that the interface roughness, $w(t)$, follows a scaling function of the form

$$w(L,t) \sim L^{\alpha} f(t/L^{z})\,, \tag{1}$$

where L is the system size and α and z are characteristic scaling exponents.[1] In general, two scaling regimes are found depending on the argument u of the function f. For $u \ll 1$ $f(u) \sim u^{\beta}$ (with $\beta = \alpha/z$) and $f(u) = \text{const}$ for $u \gg 1$. In turn, the values of the scaling exponents (α, β and z) are used to identify several universality classes for the roughening processes. In particular, much attention has been specially paid to surface growth via molecular beam epitaxy (MBE).[2] Ideally, MBE growth is conservative with no desorption and no surface overhangs allowed, which is known as the solid-on-solid (SOS) condition. The chemical-bonding environment is considered in establishing the deposition rules, which means that freshly landed particles relax into local energy minima which are defined according to the interactions among particles. In this paper we address the question of the scaling properties in some discrete models developed to mimic MBE and discuss a real case. We have found that scaling is not the rule but the exception.

2. Continuum and Discrete Approaches

Continuous growth models in the SOS approach must obey a mass conservation law that leads to the continuity equation

$$\frac{\partial h(x,t)}{\partial t} = \nabla j(x,t) + \eta\,. \tag{2}$$

Several processes give rise to different dependencies of the surface current, $j(x,t)$, on $h(x,t)$, $dh(x,t)/dt$, etc. However, in many models $j(x,t)$ is considered to be driven by the gradient of a local chemical potential

$$j(x,t) \sim \nabla u(x,t)\,. \tag{3}$$

With Eqs. (2) and (3), the growth equation for SOS models adopts the form

$$\frac{\partial h(x,t)}{\partial t} = \nu \nabla^{2} u(x,t) + \eta\,. \tag{4}$$

From a different perspective, discrete growth models address the question from an atomistic point of view by taking into account deposition and atomic diffusion mechanisms. In SOS models incident atoms stick only at the tops of substrate atoms and the resulting growing structure is a lattice of columns whose heights increase as matter is added. Discrete models have been studied mainly using computer simulations because a variety of rules are not difficult to be established. However, the analysis of the results has been shown not to be a simple task.[4]

Discrete models that emphasize the role of chemical bonding in the relaxation process have been proposed by Wolf and Villain (WV) and Das Sarma and Tamborenea (DT) independently. They proposed two models which, at first sight, only differ slightly.[5,6] WV and DT models are considered to be suitable to represent MBE processes. During MBE the gravitational force is negligible compared to the binding forces acting on particles at the surface and then it is very reasonable to assume that particles tend to end their diffusion at sites with a high binding energy (a large number of neighbors). In both models particles are dropped at randomly chosen positions. Subsequently, just-dropped particles can remain where they were deposited or relax to nearby sites by moving left or right one site. In the DT model, a just-deposited particle having only one neighbor can choose a neighbor site with a larger number of neighbors, while in the WV model a just-deposited particle relaxes toward the neighbor site having the larger number of neighbors.

There have been several attempts to establish the equivalence between discrete growth models and continuum growth equations. Most of the work has been done numerically by comparing the simulated exponents of the discrete models with those for the continuum equations. For the DT and WV models it was originally found that α and β had values coincident with the exponents predicted by the following stochastic growth equation of the Mullins–Herring type:

$$\frac{\partial h(x,t)}{\partial t} = -\nu\nabla^4 h(x,t) + \eta\,. \qquad (5)$$

The linear term in this equation can be understood as the tendency for particles to stick at kink sites. From Eqs. (4) and (5) it can be seen that the chemical potential is directly related to the local radius of curvature of the surface. Therefore, with the linear term in Eq. (5), it is assumed that the chemical potential is lower if the radius of curvature is positive and small. Equation (5) can be solved exactly and the exponents were deduced to be $\alpha = 3/2$ and $\beta = 3/8$ in $1+1$ dimensions.[1] (More recently it has been proposed that the WV and DT models belong to different universality classes.[7])

From the direct simulation of discrete models, the scaling exponents can be determined from the basic relations $w(t) \sim t^{\beta}$ before the roughness saturation is reached and $w(L) \sim L^{\alpha}$ after saturation. However, Wolf and coworkers resort to the behavior of the structure factor being much more sensitive. The structure factor is defined as

$$S(k,t) = \langle h(k,t)h(-k,t)\rangle\,, \qquad (6)$$

where

$$h(k,t) = \frac{1}{L^{1/2}}\sum [h(x,t) - \overline{h}]\exp(ikx)\,. \qquad (7)$$

The roughness scaling hypothesis reflects into the structure factor as[1]

$$S(k,t) = k^{-d-2\alpha} g(t/k^{-z})\,. \qquad (8)$$

In particular, note that the roughness scaling implies that $S(k,t)$ *is not a function of the lattice size* L. In steady state, $t \to \infty$, the function $g(.)$ is constant and then $S(k,t) \sim k^{-d-2\alpha}$, where d is the lattice dimension.

3. Discrete Models and Particle Interactions

As described above, in the WV model, particles choose sites with the largest number of neighbors. For the WV model it was originally found that $\alpha = 1.4 \pm 0.1$ and $\beta = 0.365 \pm 0.015$.[5] These values are quite close to $\alpha = 3/2$ and $\beta = 3/8$ predicted by Eq. (5). However, it has been argued that the Wolf–Villain and related models do not obey the scaling hypothesis. Indeed, Wolf himself, using the steady-state structure factor, showed that the WV model has no self-affine scaling and proposed a modification of the scaling function for his model.[8]

Later, Kim and Das Sarma introduced a model known as the larger curvature (LC) model, in which, in relaxing, particles must choose the site with the highest value of, i.e. with larger curvature.[9] They

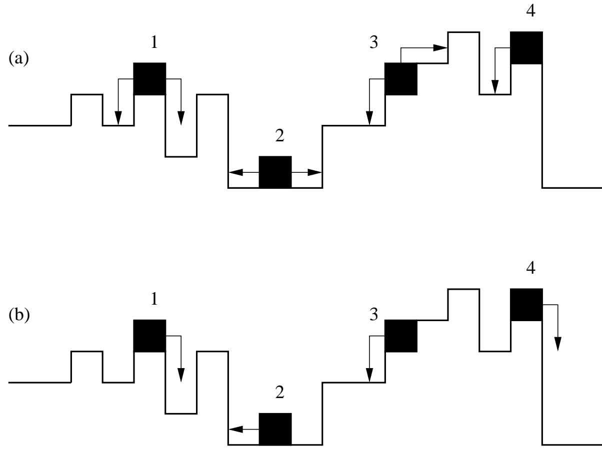

Fig. 1. Several examples for the relaxation processes in the Wolf–Villain model (a) and the large curvature model (b).

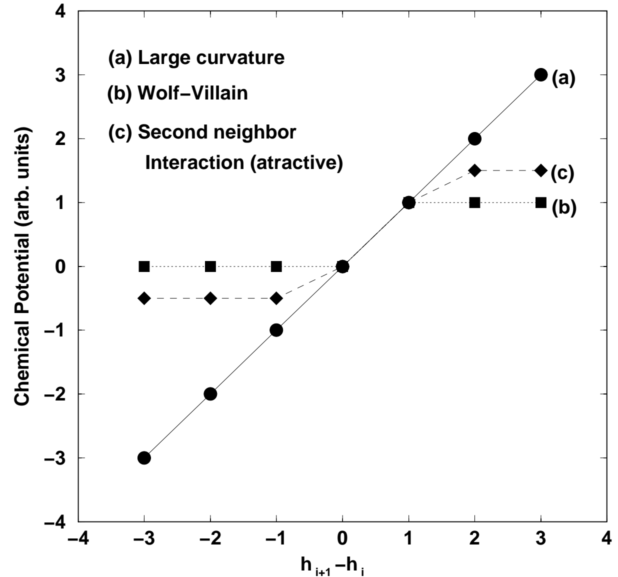

Fig. 2. The contribution of the right kink size to the chemical potential in the large curvature model, the Wolf–Villain model, and a model which includes attractive interactions with second neighbors.

adopted a finite-difference approximation to evaluate the second derivative as in Eq. (5). This is not what is done in WV or DT models.

In Fig. 1 the relaxation mechanisms in the WV and LC models are depicted for the same structure. We have specially chosen some cases for which the particles relax in a different manner. Note that in the WV model relaxation occurs regardless of the difference between heights involved. In the LC model the heights of columns determine the value of $\nabla^2 h(x,t)$. Particles 1, 2 and 3 in the WV model choose indistinctly to relax to the left or to the right because of the same number of first neighbors, but in the LC model there is one specific site where the just arriving particle chooses to diffuse. Interestingly, particle 4 relaxes by diffusing to opposite sites, depending on the model. It is clear that the WV model *cannot be considered a discretization* of the relaxation mechanism represented by $\nabla^4 h(x,t)$. Conversely, the LC model is a discrete version of the relaxation included in Eq. (5), and thus one would expect a good correspondence with its resulting surface roughening.

From an atomistic point of view, the LC model is far from being realistic because it implies interactions that do not depend on the distance between the particles involved. Indeed, the chemical potential is determined by the second derivative that proportionally depends on the height differences between neighbor columns, i.e. adding a particle on a neighbor site affects the chemical potential for a site independently of the kink size. This becomes apparent if $\nabla^2 h$ is discretized as

$$\nabla^2 h = [h(i-1) - h(i)] + [h(i+1) - h(i)]\,, \qquad (9)$$

where now the second derivative at a given site, and then the chemical potential, is directly expressed as the sum of the kink sizes on the left and right. In Fig. 2 we can see the contribution of the right kink size to the chemical potential for the LC and WV models up to kinks of size 3.

Finally, we mention a model introduced by Ryu and Kim that is a natural extension of the WV model in which second neighbor interactions are included.[10] We also present here results corresponding to second neighbor repulsive interactions not studied in Ref. 10. Figure 2 shows the resulting contribution of the right kink size to the chemical potential when second neighbor interactions are positive and a half of that corresponding to first neighbors. Interestingly, the structure factor for this model shows a better scaling than that for the WV model as shown in Fig. 3, i.e. with the inclusion of attractive second neighbor interactions the model behaves closer to the LC model. As farther neighbors of the contiguous columns are taken into account, the chemical potential better resembles the LC model and we found that the resulting model exhibits a better scaling.

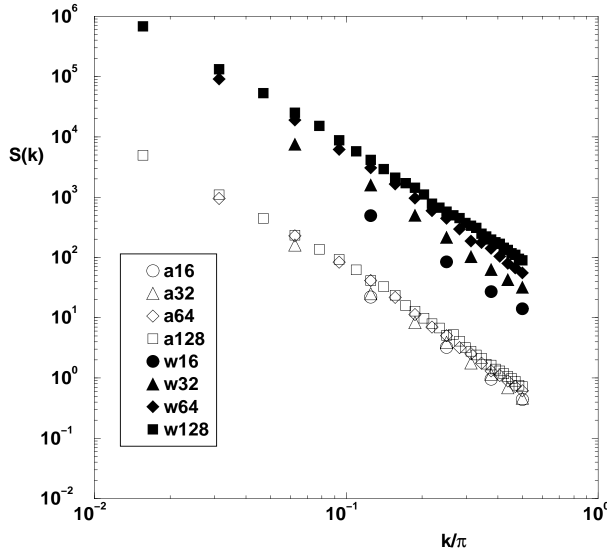

Fig. 3. Steady-state structure factor, $S(k)$, for the WV model (filled symbols) and for a model that includes attractive interactions with second neighbors (empty symbols). w16, w32, w64 and w128 refer to the WV model for $L = 16$, 32, 64 and 128, respectively. a16, a32, a64 and a128 refer to the model with interactions up to second neighbors for $L = 16$, 32, 64 and 128, respectively. For the sake of clarity, $S(k)$ for the WV model is displayed shifted up by an order of magnitude.

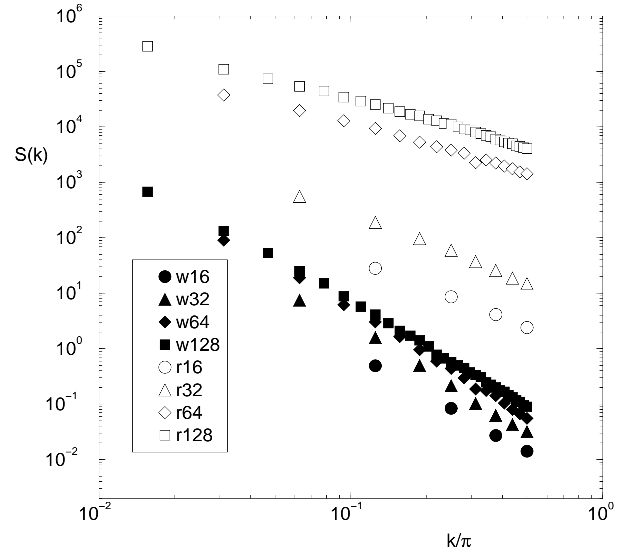

Fig. 4. Steady-state structure factor, $S(k)$, for the WV model (filled symbols) and for a model that includes repulsive interactions with second neighbors (empty symbols). w16, w32, w64 and w128 refer to the WV model for $L = 16$, 32, 64 and 128, respectively. r16, r32, r64 and r128 refer to the model with interactions up to second neighbors for $L = 16$, 32, 64 and 128, respectively. For the sake of clarity, $S(k)$ for the WV model is displayed shifted down by two orders of magnitude.

As can be seen in Fig. 4, if second neighbor interactions are of the repulsive type, the resulting interface roughness clearly does not scale; the structure factor becomes more strongly dependent on L. Even worse, the exponent α deduced from $S(k)$ depends on the chosen value of L. For instance, the value of α, calculated from the slope of $S(k)$, for $L = 128$ is 0.11 while for $L = 16$ it is 0.38. On the other hand, if α is calculated from the roughness under saturation conditions (plots not shown), it is found to be greater than 2.

4. Roughening of Si(100) Steps During Homoepitaxial Growth

The most pronounced feature of Si(100) is that it forms parallel rows of dimerized atoms. These rows are orthogonal on adjacent atomic terraces, giving rise to alternating 2×1 and 1×2 domains. Step edges aligned parallel to the dimer rows of the upper terrace are denoted as S_A, and step edges perpendicular to the upper terrace dimer rows are denoted as S_B. Consistent with the energetically favorable way in which the ends of dimer rows terminate on the lower terrace,[11,12] S_B step edges tend to offset by an even number of dimers. The configurations of these steps have attracted considerable interest because of their role in crystal growth, epitaxy, and etching.[13–19]

Wu *et al.*[20] reported a very interesting study for kinetic roughening and finger formation in steps of Si(100) miscut toward [100] during homoepitaxial growth. Because of the high anisotropy in diffusion, an adatom landing on a particular dimer row would diffuse preferentially along the row and would eventually arrive at one of the ends. Adatoms arriving at S_B steps fall over the step and can be incorporated into the step, while atoms arriving at S_A steps are reflected. Thus adatoms deposited on a particular dimer row tend to extend that row at its down-step end. The longer the row, the more it is able to collect deposited atoms. Fluctuations present in the equilibrium pattern or in the flux of arriving atoms will cause some rows to grow more quickly than others and, subsequently, to collect even more atoms.

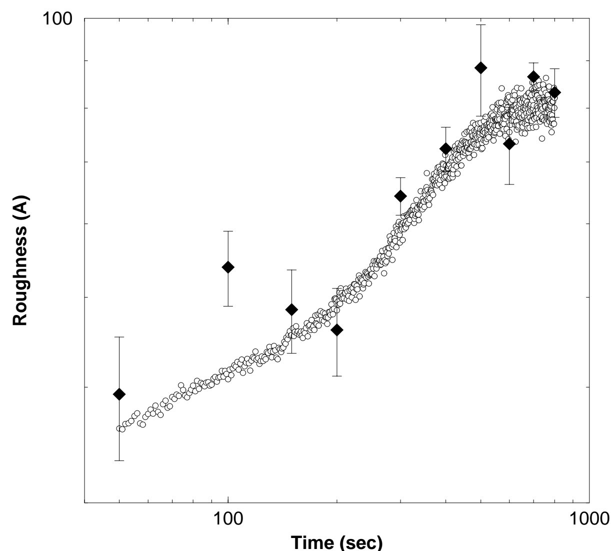

Fig. 5. Roughness as a function of time for a model that mimics the roughening of Si(100) steps during homoepitaxial growth. Experimental points were extracted from Ref. 20.

This implies a positive feedback that would produce fingers.

The discussion above is correct but an important point must be taken into account: rows do not directly collect individual atoms arriving to their ends. Since kinks in monatomic step edges on vicinal Si(100) present mostly a length corresponding to an integer number of dimer rows, fluctuations must occur dominantly through the attachment and detachment of sets of two dimers, as has been confirmed by STM observations.[16] Then, the attaching of a block involves four atoms and intermediate structures have very short lifetimes. Since blocks (not atoms) are the stable attaching "particles", "block events" need to be modeled. In doing so, the atom deposition influence on block attaching at step edges has to be incorporated. Based on this kind of known mechanisms present in homoepitaxial Si growth, we introduced a model that leads to the observed fingerlike configurations and their evolution.[21] In Fig. 5 we show the roughness as a function of time for this model including the experimental results extracted from Ref. 20. The time evolution of the roughness shows an initial slow increase that can be understood as an effect of the positive feedback. This is, some roughness involving short and long rows is needed for the positive feedback to act. This explains an increasing delay, observed in experiments, for the onset of fingering as the temperature is raised.

Thus, comparison to experimental findings indicates that dendrite-like fingers are the result of a positive feedback due to the well-known diffusional anisotropy in Si(100) within a solid-on-solid model. This specific example shows that real growing interfaces can be much more complex than theoretical models as the WV or DT models. Clearly, as shown in Fig. 5, the time evolution of the roughness is far from showing scaling properties.

5. Final Remarks

Continuum models of deposition processes are only approximations to reality because the surface of a crystal is discrete, since it is made up of individual atoms. Thus, the height of a crystal does not change continuously but in jumps corresponding to the adding or removing of particles from the surface. In that sense, an atomistic approach is a better representation of depositions on crystals.

It is important to point out that universal scaling has been unambiguously proved only for some continuum models. In discrete models, by analyzing the behavior of the basic relations $w(t) \sim t^{\beta}$ before saturation and $w(L) \sim L^{\alpha}$ and specially $S(k,t)$ after saturation, the lack of scaling can be proved but, strictly speaking, scaling can only be conjectural.

Discrete models appear to show scaling as they are a discretization of continuum models that do scale. This is the case for the LC model, a discretization of a Mullins–Herring type equation, and for the Family–Vicsek model, a discretization of the the Edwards–Wilkinsonn equation.[14] However, in general, one should not expect that discrete models (as well as real crystals) exhibit scaling.

References

1. A.-L. Barabási and H. E. Stanley, *Fractal Concepts in Surface Growth* (University Press, Cambridge, 1995).
2. F. Family and T. Vicsek (eds.), *Dynamics of Fractal Surfaces* (World Scientific, Singapore, 1991).
3. T. Vicsek, *Fractal Growth Phenomena* (World Scientific, Singapore, 1992).
4. M. Plischke, J. D. Shore, M. Schroeder, M. Siegert and D. E. Wolf, *Phys. Rev. Lett.* **71**, 2509 (1993).
5. D. E. Wolf and J. Villain, *Europhys. Lett.* **13**, 389 (1990).

6. S. Das Sarma and P. Tamborenea, *Phys. Rev. Lett.* **66**, 325 (1991).
7. Z. Huang and B. Gu, *Phys. Rev.* **E54**, 5935 (1996).
8. M. Schroeder, M. Siegert, D. E. Wolf, J. D. Shore and M. Plischke, *Europhys. Lett.* **24**, 563 (1990).
9. J. M. Kim and S. Das Sarma, *Phys. Rev. Lett.* **72**, 2903 (1994).
10. C. S. Ryu and I. Kim, *Phys. Rev.* **E51**, 3069 (1995).
11. D. J. Chadi, *Phys. Rev. Lett.* **59**, 1691 (1987).
12. R. H. Hamers, R. M. Tromp and J. E. Demuth, *Phys. Rev.* **B34**, 5343 (1986).
13. R. Kariotis and M. G. Lagally, *Surf. Sci.* **248**, 295 (1991).
14. X. Tong and P. A. Bennett, *Phys. Rev. Lett.* **67**, 101 (1991).
15. M. B. Webb, F. K. Men, B. S. Swartzentruber, R. Kariotis and M. G. Lagally, *Surf. Sci.* **242**, 23 (1991).
16. H. J. W. Zandvliet, H. Wormeester, D. J. Wentink, A. van Silhout and H. B. Elswijk, *Phys. Rev. Lett.* **70**, 2122 (1993).
17. D. Rioux, M. Chander, Y. Z. Li and J. H. Weaver, *Phys. Rev.* **B49**, 11071 (1994).
18. H. J. W. Zandvliet, B. Poelsema and H. B. Elswijk, *Phys. Rev.* **B51**, 5465 (1995).
19. K. Cho, J. D. Joannopoulos and A. Nihat Berker, *Phys. Rev.* **B53**, 1002 (1996).
20. F. Wu, S. G. Jaloviar, D. E. Savage and M. G. Lagally, *Phys. Rev. Lett.* **71**, 4190 (1993).
21. D. A. Mirabella, F. J. Williams and C. M. Aldao, *Phys. Rev.* **B59**, 9850 (1999).
22. F. Family, *J. Phys.* **A19**, L441 (1986).
23. F. Family and T. Vicsek, *J. Phys.* **A18**, L75 (1985).

Copyright © 2002 EBSCO Publishing